Deriving the velocity distribution of Galactic dark matter particles from the rotation curve data

Pijushpani Bhattacharjee,[1,2,*] Soumini Chaudhury,[1,†] Susmita Kundu,[1,‡] and Subhabrata Majumdar[3,§]

[1]*Astroparticle Physics and Cosmology Division and Centre for Astroparticle Physics, Saha Institute of Nuclear Physics, 1/AF Bidhannagar, Kolkata 700064, India*

[2]*McDonnell Center for the Space Sciences and Department of Physics, Washington University in St. Louis, Campus Box 1105, One Brookings Drive, St. Louis, Missouri 63130, USA*

[3]*Department of Theoretical Physics, Tata Institute of Fundamental Research, Homi Bhabha Road, Mumbai 400005, India*

(Received 10 October 2012; revised manuscript received 21 January 2013; published 26 April 2013)

The velocity distribution function (VDF) of the hypothetical weakly interacting massive particles (WIMPs), currently the most favored candidate for the dark matter in the Galaxy, is determined directly from the circular speed (''rotation'') curve data of the Galaxy assuming isotropic VDF. This is done by ''inverting''—using Eddington's method—the Navarro-Frenk-White universal density profile of the dark matter halo of the Galaxy, the parameters of which are determined by using the Markov chain Monte Carlo technique from a recently compiled set of observational data on the Galaxy's rotation curve extended to distances well beyond the visible edge of the disk of the Galaxy. The derived most-likely local isotropic VDF strongly differs from the Maxwellian form assumed in the ''standard halo model'' customarily used in the analysis of the results of WIMP direct-detection experiments. A parametrized (non-Maxwellian) form of the derived most-likely local VDF is given. The astrophysical ''g factor'' that determines the effect of the WIMP VDF on the expected event rate in a direct-detection experiment can be lower for the derived most-likely VDF than that for the best Maxwellian fit to it by as much as 2 orders of magnitude at the lowest WIMP mass threshold of a typical experiment.

DOI: 10.1103/PhysRevD.87.083525 PACS numbers: 95.35.+d, 98.35.Df, 98.35.Gi

Several experiments worldwide are currently trying to directly detect the hypothetical weakly interacting massive particles (WIMPs), thought to constitute the dark matter (DM) halo of our Galaxy, by looking for nuclear recoil events due to scattering of WIMPs off nuclei of suitably chosen detector materials in low background underground facilities. The rate of nuclear recoil events depends crucially on the local (i.e., solar neighborhood) density and velocity distribution of the WIMPs in the Galaxy [1], which are *a priori* unknown. Estimates based on a variety of observational data typically yield values for the local density of DM, $\rho_{\mathrm{DM},\odot}$, in the range 0.2–0.4 GeV cm^{-3} [$(0.527\text{–}1.0)\times 10^{-2} M_\odot$ pc^{-3}] [2]. In contrast, not much knowledge directly based on observational data is available on the likely form of the velocity distribution function (VDF) of the WIMPs in the Galaxy. The standard practice is to use what is often referred to as the ''standard halo model'' (SHM), in which the DM halo of the Galaxy is described as a single-component isothermal sphere [3], for which the VDF is assumed to be isotropic and of Maxwell-Boltzmann (hereafter simply ''Maxwellian'') form, $f(\mathbf{v}) \propto \exp(-|\mathbf{v}|^2/v_0{}^2)$, with a truncation at an assumed value of the local escape speed, and with $v_0 = v_{c,\odot}$, the circular rotation velocity at the location of the Sun. Apart from several theoretical issues (see, e.g., Ref. [4]) concerning the self-consistency of the SHM as a model of a finite-size, finite-mass DM halo of the Galaxy, high resolution cosmological simulations of DM halos [5] give strong indications of significant departure of the VDF from the Maxwellian. On the other hand, these cosmological simulations do not yet satisfactorily include the gravitational effects of the visible matter (VM) components of the real Galaxy, namely, the central bulge and the disk, which provide the dominant gravitational potential in the inner regions of the Galaxy including the solar neighborhood region.

The VDF of the DM particles at any location in the Galaxy is self-consistently related to their spatial density as well as to the *total* gravitational potential, $\Phi(\mathbf{x})$, at that location. For a spherical system of collisionless particles (WIMPs, for example) with isotropic VDF satisfying the collisionless Boltzmann equation, the Jeans theorem [3] ensures that the phase space distribution function $\mathcal{F}(\mathbf{x}, \mathbf{v})$ depends on the phase space coordinates $(\mathbf{x}, \mathbf{v})$ only through the total energy (per unit mass), $E = \frac{1}{2}v^2 + \Phi(r)$, where $v = |\mathbf{v}|$, $r = |\mathbf{x}|$. For such a system, given a isotropic spatial density distribution $\rho(r) \equiv \int d^3\mathbf{v}\mathcal{F}(E)$, one can get a unique $\mathcal{F}$ by the Eddington formula [3,6]

$$\mathcal{F}(\mathcal{E}) = \frac{1}{\sqrt{8}\pi^2}\left[\int_0^{\mathcal{E}} \frac{d\Psi}{\sqrt{\mathcal{E}-\Psi}}\frac{d^2\rho}{d\Psi^2} + \frac{1}{\sqrt{\mathcal{E}}}\left(\frac{d\rho}{d\Psi}\right)_{\Psi=0}\right], \quad (1)$$

where $\Psi(r) \equiv -\Phi(r) + \Phi(r=\infty)$ is the relative potential and $\mathcal{E} \equiv -E + \Phi(r=\infty) = \Psi(r) - \frac{1}{2}v^2$ is the relative energy, with $\mathcal{F} > 0$ for $\mathcal{E} > 0$, and $\mathcal{F} = 0$ for $\mathcal{E} \le 0$.

*pijush.bhattacharjee@saha.ac.in
†soumini.chaudhury@saha.ac.in
‡susmita.kundu@saha.ac.in
§subha@tifr.res.in

 © 2013 American Physical Society

The latter condition implies that at any location r, the VDF $f_r(\mathbf{v}) = \mathcal{F}/\rho(r)$ has a natural truncation at a maximum value of v, namely, $v_{\rm max}(r) = \sqrt{2\Psi(r)}$.

Thus, given a isotropic density profile of a set of collisionless particles, we can calculate the VDF, $f_r(\mathbf{v})$, using Eq. (1) provided the total gravitational potential $\Phi(r)$ in which the particles move is known. A direct observational probe of $\Phi(r)$ is provided by the rotation curve (RC) of the Galaxy, the circular velocity of a test particle as a function of the galactocentric distance. In this paper we reconstruct the total gravitational potential $\Phi(r)$ in the Galaxy directly from the Galactic RC data and then use Eq. (1) to obtain the VDF, $f_r(\mathbf{v})$, of the WIMPs at any location in the Galaxy [7].

We shall assume that the DM density profile to be used on the right-hand side of Eq. (1) is of the universal Navarro-Frenk-White [9] form, which, when normalized to DM density at solar location, can be written as

$$\rho_{\rm DM}(r) = \rho_{\rm DM,\odot}\left(\frac{R_0}{r}\right)\left(\frac{r_s + R_0}{r_s + r}\right)^2, \tag{2}$$

where R_0 is the distance of the Sun from the Galactic center. The profile given by Eq. (2) has two free parameters, namely, the density $\rho_{\rm DM,\odot}$ and the scale radius r_s.

The *total* gravitational potential seen by the DM particle, Φ, is given by $\Phi = \Phi_{\rm DM} + \Phi_{\rm VM}$, where $\Phi_{\rm DM}$ is the DM potential corresponding to the density distribution given by Eq. (2) and $\Phi_{\rm VM}$ is the total potential due to the VM component of the Galaxy. The latter can be effectively modeled [10] in terms of a spheroidal bulge superposed on an axisymmetric disk, with density distributions given, respectively, by $\rho_b = \rho_{\rm b0}(1 + (r/r_{\rm b})^2)^{-3/2}$, where $\rho_{\rm b0}$ and $r_{\rm b}$ are the central density and scale radius of the bulge, respectively, and $\rho_d(R, z) = \frac{\Sigma_\odot}{2z_{\rm d}} e^{-(R-R_0)/R_{\rm d}}\, e^{-|z|/z_{\rm d}}$, where R and z are the axisymmetric cylindrical coordinates with $r = (R^2 + z^2)^{1/2}$, $R_{\rm d}$ and $z_{\rm d}$ are the scale length and scale height of the disk, respectively, and $\Sigma_\odot$ is its local surface density. The corresponding gravitational potentials for these density models, $\Phi_{\rm bulge}$ and $\Phi_{\rm disk}$, can be easily obtained by numerically solving the respective Poisson equations, thus giving $\Phi_{\rm VM} = \Phi_{\rm bulge} + \Phi_{\rm disk}$.

The density models specified above have a total of seven free parameters, namely, r_s, $\rho_{\rm DM,\odot}$, $\rho_{\rm b0}$, $r_{\rm b}$, $\Sigma_\odot$, $R_{\rm d}$, and $z_{\rm d}$. We determine the most-likely (ML) values and the 68% C.L. upper and lower ranges of these parameters by performing a Markov chain Monte Carlo (MCMC) analysis (see, e.g., Ref. [11]) using the observed RC data of the Galaxy. For a given set of the Galactic model parameters, the circular rotation speed, $v_c(R)$, as a function of the galactocentric distance R, is given by

$$v_c^2(R) = R\frac{\partial}{\partial R}[\Phi_{\rm DM}(R, z = 0) + \Phi_{\rm VM}(R, z = 0)]. \tag{3}$$

For the observational data, we use a recently compiled set of RC data [12] that extends to galactocentric distances well beyond the visible edge of the Galaxy. This data set corresponds to a choice of the local standard of rest (LSR) set to $(R_0, v_{c,\odot}) = (8.0\,{\rm kpc}, 200\,{\rm km\,s^{-1}})$ [13]. For the MCMC analysis, we use the χ^2-test statistic defined as $\chi^2 \equiv \sum_{i=1}^{i=N}(\frac{v^i_{\rm c,obs} - v^i_{\rm c,th}}{v^i_{\rm c,error}})^2$, where $v^i_{\rm c,obs}$ and $v^i_{\rm c,error}$ are, respectively, the observational value of the circular rotation speed and its error at the ith value of the galactocentric distance, and $v^i_{\rm c,th}$ is the corresponding theoretically calculated circular rotation speed. For priors on the free parameters involved, we have taken the following ranges of the relevant parameters based on currently available observational knowledge: For the VM parameters, $\rho_{\rm b0}$: [0.1–2] $\times$ $4.2 \times 10^2 M_\odot\,{\rm pc}^{-3}$ [10]; $r_{\rm b}$: [0.01–0.2] $\times$ 0.103 kpc [10]; $\Sigma_\odot$: [35–58]$M_\odot\,{\rm pc}^{-2}$ [14]; $R_{\rm d}$: [1.7–3.5] kpc [10,15]. The parameter $z_{\rm d}$ has been fixed at 340 pc [16] since the results are fairly insensitive to this parameter. For the DM parameters we took a wide enough prior range for r_s: [0.1–100] kpc and $\rho_{\rm DM,\odot}$: [0.1–0.5] GeV cm^{-3} consistent with values recently quoted in the literature [2].

The results of our MCMC analysis are summarized in Table I and Fig. 1. Figure 2 shows the theoretically calculated rotation curve for the most-likely set of values of the Galactic model parameters obtained from the MCMC analysis and listed in Table I, and its comparison with the observed rotation curve data. In Table II, we display the values of some of the physical quantities of interest characterizing the Galaxy, derived from the Galactic parameters listed in Table I. The values in Table II are in reasonably good agreement with the values of these quantities quoted in recent literature [8,12,17]. The relatively large uncertainties in the values of some of the quantities

TABLE I. The most-likely values of the Galactic model parameters, as well as their 68% C.L. lower and upper ranges, means and standard deviations, obtained from our MCMC analysis using the observed rotation curve data.

Parameter	r_s (kpc)	$\rho_{\rm DM,\odot}$ (GeV/cm^3)	$\rho_{\rm b0} \times 10^{-4}$ (GeV/cm^3)	$r_{\rm b}$ (kpc)	$\Sigma_\odot$ ($M_\odot$/pc^2)	$R_{\rm d}$ (kpc)
Most-likely	30.36	0.19	1.83	0.092	57.9	3.2
Lower	14.27	0.17	1.68	0.083	55.51	2.99
Upper	53.37	0.23	2.0	0.102	58.0	3.27
Mean	41.35	0.20	1.84	0.092	54.30	3.14
Standard deviations	20.51	0.02	0.059	0.001	3.47	0.11

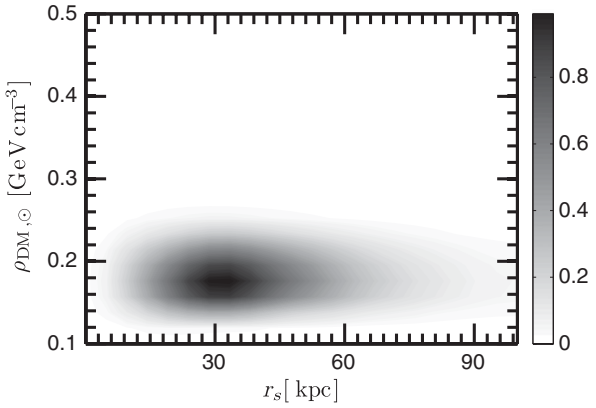

FIG. 1. The 2D posterior probability density function for dark matter parameters ($r_s - \rho_{DM,\odot}$), marginalized over the visible matter parameters.

that receive dominant contribution from the DM halo properties at large galactocentric distances are simply a reflection of the relatively large uncertainties of the rotation curve data at those distances.

The Galactic model parameters determined above allow us to reconstruct the total gravitational potential $\Phi(\mathbf{x})$ at any location in the Galaxy. Because of the axisymmetric nature of the VM disk, this potential is nonspherical. To use Eq. (1), which is valid only for a spherically symmetric situation, we use the spherical approximation [8,18], $\Phi_{VM}(r) \simeq G\int_0^r M_{VM}(r')/r'^2 dr'$, where M_{VM} is the total VM mass contained within r [19].

The resulting normalized speed distribution $f_r(v) \equiv (4\pi v^2) f_r(\mathbf{v})$ [with $\int f_r(v)dv = 1$] evaluated at the location of the Sun, giving the most-likely $f_\odot(v)$, is shown in Fig. 3. For comparison, we also show in the same figure the best Maxwellian fit (BMF) [with $f_\odot^{\rm Maxwell}(v) \propto v^2 \exp(-v^2/v_0^2)$] to the most-likely $f_\odot(v)$ obtained from MCMC analysis. We also compare our results with those from four large N-body simulations [5].

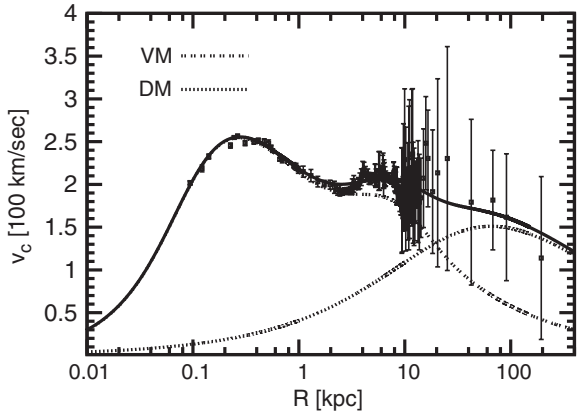

FIG. 2. Rotation curve of the Galaxy with the most-likely set of values of the Galactic model parameters listed in Table I. The data with error bars are from Ref. [12].

TABLE II. The most-likely values of various relevant physical parameters of the Milky Way and their upper and lower ranges derived from the most-likely and 68% C.L. upper and lower ranges of values of the Galactic model parameters listed in Table I.

Derived quantities	Unit	Values
Bulge mass (M_b)	$10^{10}M_\odot$	$3.53^{+1.81}_{-1.29}$
Disk mass (M_d)	$10^{10}M_\odot$	$4.55^{+0.2}_{-0.22}$
Total VM mass ($M_{VM} = M_b + M_d$)	$10^{10}M_\odot$	$8.07^{+2.01}_{-1.51}$
DM halo virial radius (r_{vir})	kpc	$199.0^{+75}_{-53.5}$
Concentration parameter ($\frac{r_{vir}}{r_s}$)	...	$6.55^{+5.01}_{-2.05}$
DM halo virial mass (M_h)	$10^{11}M_\odot$	$8.61^{+14.01}_{-5.22}$
Total mass of Galaxy ($M_{VM} + M_h$)	$10^{11}M_\odot$	$9.42^{+14.21}_{-5.37}$
DM mass within R_0	$10^{10}M_\odot$	$1.89^{+0.72}_{-0.3}$
Total mass within R_0	$10^{10}M_\odot$	$7.09^{+1.9}_{-1.15}$
Total surface density at $R_0(\lvert z\rvert \le 1.1$ kpc)	$M_\odot$ pc^{-2}	$69.21^{+2.52}_{-3.55}$
Total mass within 60 kpc	$10^{11}M_\odot$	$3.93^{+2.15}_{-1.41}$
Total mass within 100 kpc	$10^{11}M_\odot$	$5.92^{+4.35}_{-2.56}$
Local circular velocity ($v_{c,\odot}$)	km s^{-1}	$206.47^{+24.67}_{-16.3}$
Local maximum velocity ($v_{max,\odot}$)	km s^{-1}	$516.02^{+120.85}_{-97.58}$

As evident from Fig. 3, the speed distribution differs significantly from the Maxwellian form. We find that the following parametrized form, which goes over to the standard Maxwellian form in the limit of the parameter $k \to 0$,

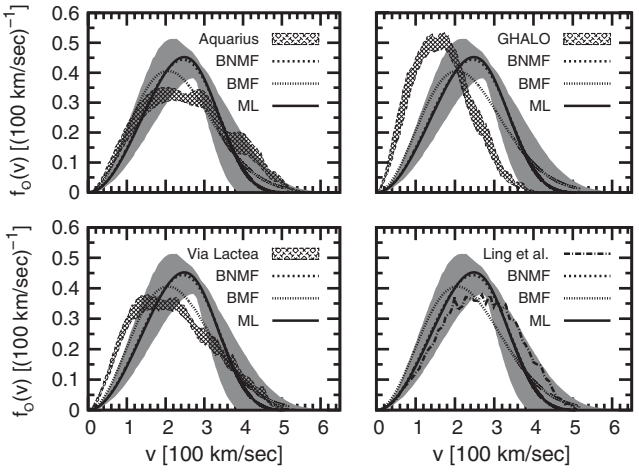

FIG. 3. Normalized local speed distribution $f_\odot(v)$ corresponding to the ML set of values of the Galactic model parameters given in Table I (solid curve) and its uncertainty band (shaded) corresponding to the 68% C.L. upper and lower ranges of the Galactic model parameters. The four panels show comparison of our results with those from four different N-body simulations [5], as indicated. In each panel, the best non-Maxwellian fit (BNMF) [Eq. (4)—almost indistinguishable from the ML curve] as well as the BMF, the latter with the form $f_\odot^{\rm Maxwell}(v) \propto v^2 \exp(-v^2/v_0^2)$ truncated at $v_{max,\odot} = 516\,\mathrm{km\,s^{-1}}$ (see Table II) and with the free parameter v_0 determined to be 206 km s^{-1}, are also shown.

gives a good fit to our numerically obtained most-likely local speed distribution shown in Fig. 3:

$$f_\odot(v) \approx 4\pi v^2(\xi(\beta) - \xi(\beta_{\rm max})), \tag{4}$$

where $\xi(x) = (1+x)^k e^{-x^{(1-k)}}$, $\beta = v^2/v_0^2$, $\beta_{\rm max} = v_{{\rm max},\odot}^2/v_0^2$, $v_0 = 339$ km s^{-1}, and $k = -1.47$. As a quantitative measure of the deviation of a model form of the local speed distribution, $f^{\rm model}$, from the numerically obtained ML form $f^{\rm ML}$ shown in Fig. 3, the quantity $\chi_f^2 \equiv (1/N)\sum_{i=1}^{N}[f^{\rm ML}(v_i) - f^{\rm model}(v_i)]^2$ has a value of $\sim 7.2 \times 10^{-5}$ for the parametrized form given by Eq. (4) compared to a value $\sim 1.7 \times 10^{-3}$ for the best Maxwellian fit shown in Fig. 3. Note also that our results differ significantly from those obtained from the N-body simulations.

In Fig. 4 we show the most-likely $f_r(v)$'s at several different values of the galactocentric distance r. Notice how the peak of the distribution shifts towards smaller values of v and the width of the distribution shrinks, as we go to larger r, with the distribution eventually becoming a delta function at zero speed at asymptotically large distances, as expected. The non-Maxwellian nature of the distribution at all locations is also clearly seen, with the Maxwellian approximation always overestimating the number of particles at both low as well as extreme high velocities. The inset in Fig. 4 shows our results for the pseudophase space density, $Q \equiv \rho/\langle v^2\rangle^{3/2}$, as a function of r, and its comparison with the power-law behavior predicted from simulation results [20]. Note the agreement with the power-law behavior at large distances but strong deviation from it at smaller galactocentric radii, which we attribute to the effect of the visible matter: For a given DM density profile, the additional gravitational potential provided by the VM supports higher velocity dispersion

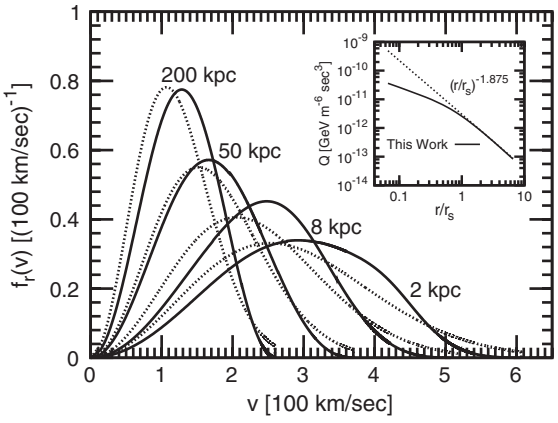

FIG. 4. Normalized speed distribution of the DM particles at various galactocentric radii (solid curves), corresponding to the most-likely set of values of the Galactic model parameters given in Table I. The curves (dotted) for the corresponding best Maxwellian fit are also shown for comparison. The inset shows the pseudophase space density of DM, $Q \equiv \rho/\langle v^2\rangle^{3/2}$, as a function of r.

of the DM particles, making Q smaller than that for the DM-only case.

We now discuss the implications of our results for the analysis of direct-detection experiments. The differential rate of nuclear recoil events per unit detector mass (typically measured in counts/day/kg/keV), in which a WIMP (hereafter generically denoted by χ with mass m_χ) elastically scatters off a target nucleus of mass m_N leaving the recoiling nucleus with a kinetic energy E_R, can be written as [1]

$$\frac{d\mathcal{R}}{dE_R}(E_R, t) = \frac{\sigma(q^2 = 2m_N E_R)}{2m_\chi \mu^2}\rho_\chi g(E_R, t), \tag{5}$$

where $\rho_\chi \equiv \rho_{{\rm DM},\odot}$ is the local mass density of WIMPs, $\sigma(q^2)$ is the momentum transfer dependent effective WIMP-nucleus elastic cross section, $\mu = m_\chi m_N/(m_\chi + m_N)$ is the reduced mass of the WIMP-nucleus system, and

$$g(E_R, t) = \int_{u > u_{\rm min}(E_R)}^{u_{\rm max}(t)} \frac{d^3\mathbf{u}}{u} f_\odot(\mathbf{u} + \mathbf{v}_{\rm E}(\mathbf{t}))\Theta(u_{\rm max} - u_{\rm min}), \tag{6}$$

is the crucial "g factor" that contains all information about the local VDF of the WIMPs [21]. In Eq. (6) the variable $\mathbf{u}$ (with $u = |\mathbf{u}|$) represents the relative velocity of the WIMP with respect to the detector at rest on Earth, and $\mathbf{v}_{\rm E}(\mathbf{t})$ is the (time-dependent) velocity of Earth relative to the Galactic rest frame. The quantity $u_{\rm min}(E_R) = (m_N E_R/2\mu^2)^{1/2}$ is the minimum WIMP speed required for giving a recoil energy E_R to the nucleus, and $u_{\rm max}(t)$ is the (time-dependent) maximum WIMP speed [4] corresponding to the maximum speed $v_{\rm max}$ (defined in the Galactic rest frame) for the VDF under consideration.

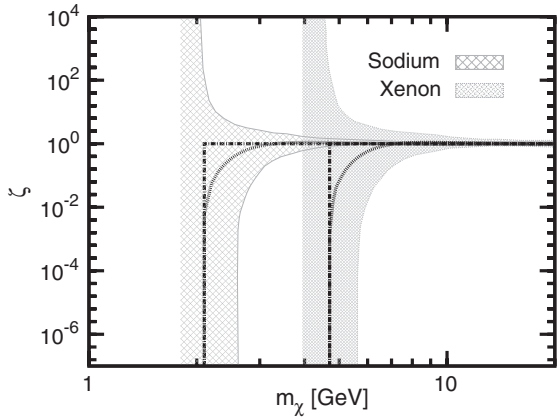

FIG. 5. The ratio (solid curves), $\zeta \equiv g_{\rm ML}(E_{\rm th})/g_{\rm Maxwell}(E_{\rm th})$, of the g factor calculated with our ML form of $f_\odot(v)$ shown in Fig. 3 to that for the best Maxwellian fit to it also shown in Fig. 3, as a function of the WIMP mass m_χ, for two different target nuclei, namely, sodium and xenon, both with $E_{\rm th} = 2$ keV. The shaded bands correspond to the uncertainty bands of $f_\odot(v)$ shown in Fig. 3. The calculations are for June 2, when Earth's velocity in the Galactic rest frame is maximum.

Note that the quantity $g(E_R, t)$ takes its largest value at $E_R = E_{\rm th}$, the threshold energy for the experiment under consideration. To illustrate the effect of the non-Maxwellian nature of the VDF and its uncertainty, we define the quantity $\zeta \equiv g_{\rm ML}(E_{\rm th})/g_{\rm Maxwell}(E_{\rm th})$, the ratio of the g factor calculated with our ML form of $f_\odot(v)$ shown in Fig. 3 to that for the best Maxwellian fit to it also shown in Fig. 3, both evaluated at $E_R = E_{\rm th}$. A plot of ζ as a function of the WIMP mass m_χ, for two different target nuclei, viz. sodium and xenon, in both case with $E_{\rm th} =$ 2 keV, is shown in Fig. 5.

The lowest WIMP mass that can be probed by a given experiment is given by $m_{\chi,\rm min} = m_N[(2m_N(v_{\rm max,\odot} + v_{\rm E})^2/E_{\rm th})^{1/2} - 1]^{-1}$. As seen from Fig. 5, the effect of the departure from Maxwellian distribution is most significant at the lowest WIMP mass where the difference can be as much as 2 orders of magnitude.

To summarize, a first attempt has been made to derive the velocity distribution (assumed isotropic) of the dark matter particles in the Galaxy directly using the rotation curve data. The distribution is found to be significantly non-Maxwellian in nature, the implication of which is a sizable deviation of the expected direct-detection event rates from those calculated with the usual Maxwellian form.

We thank Satej Khedekar and Subir Sarkar for useful discussions. P. B. thanks Ramanath Cowsik for discussions and for support under the Clark Way Harrison Visiting Professorship program at the McDonnell Center for the Space Sciences at Washington University in St. Louis.

[1] G. Jungman, M. Kamionkowski, and K. Griest, Phys. Rep. **267**, 195 (1996); J. D. Lewin and R. F. Smith, Astropart. Phys. **6**, 87 (1996).
[2] J. H. Oort, Bull. Astron. Inst. Neth. **6**, 249 (1932); **15**, 45 (1960); J. N. Bahcall, Astrophys. J. **276**, 169 (1984); P. Salucci, F. Nesti, G. Gentile, and C. F. Martins, Astron. Astrophys. **523**, A83 (2010); R. Catena and P. Ullio, J. Cosmol. Astropart. Phys. 08 (2010) 004; J. Bovy and S. Tremaine, Astrophys. J. **756**, 89 (2012).
[3] J. Binney and S. Tremaine, *Galactic Dynamics* (Princeton University, Princeton, NJ, 2008), 2nd ed.
[4] S. Chaudhury, P. Bhattacharjee, and R. Cowsik, J. Cosmol. Astropart. Phys. 09 (2010) 020; S. Kundu and P. Bhattacharjee, Phys. Rev. D **85**, 123533 (2012).
[5] J. Stadel, D. Potter, B. Moore, J. Diemand, P. Madau, M. Zemp, M. Kuhlen, and V. Quilis (GHALO simulation), Mon. Not. R. Astron. Soc. **398**, L21 (2009); J. Diemand, M. Kuhlen, P. Madau, M. Zemp, B. Moore, D. Potter, and J. Stadel (Via Lactea simulation), Nature (London) **454**, 735 (2008); V. Springel, J. Wang, M. Vogelsberger, A. Ludlow, A. Jenkins, A. Helmi, J. F. Navarro, C. S. Frenk, and S. D. M. White (Aquarius simulation), Mon. Not. R. Astron. Soc. **391**, 1685 (2008); F. S. Ling, E. Nezri, E. Athanassoula, and R. Teyssier, J. Cosmol. Astropart. Phys. 02 (2010) 012.
[6] A. S. Eddington, Mon. Not. R. Astron. Soc. **76**, 572 (1916).
[7] An earlier work by Catena and Ullio [8] used Eddington's method to derive the *local* VDF from various dynamical constraints on the gross properties of the Galaxy rather than the full RC data as done here.
[8] R. Catena and P. Ullio, J. Cosmol. Astropart. Phys. 05 (2012) 005.
[9] J. F. Navarro, C. S. Frenk, and S. D. M. White, Astrophys. J. **462**, 563 (1996).
[10] J. Caldwell and J. Ostriker, Astrophys. J. **251**, 61 (1981); K. Kuijken and G. Gilmore, Mon. Not. R. Astron. Soc. **239**, 571 (1989); **239**, 605 (1989); **239**, 651 (1989); Astrophys. J. Lett. **367**, L9 (1991).
[11] A. Putze, L. Derome, D. Maurin, L. Perotto, and R. Taillet, Astron. Astrophys. **497**, 991 (2009); A. Heavens, arXiv:0906.0664v3; http://cosmologist.info/cosmomc/.
[12] Y. Sofue, Publ. Astron. Soc. Jpn. **64**, 75 (2012).
[13] The exercise done in this paper can be repeated with other choices for the LSR. However, we do not expect the qualitative nature of our results to change significantly.
[14] M. Weber and W. de Boer, Astron. Astrophys. **509**, A25 (2010).
[15] F. Hammer, M. Puech, L. Chemin, H. Flores, and M. D. Lehnert, Astrophys. J. **662**, 322 (2007).
[16] H. T. Freudenreich, Astrophys. J. **492**, 495 (1998).
[17] P. J. McMillan, Mon. Not. R. Astron. Soc. **414**, 2446 (2011); M. I. Wilkinson and N. W. Evans, Mon. Not. R. Astron. Soc. **310**, 645 (1999); W. Dehnen and J. Binney, Mon. Not. R. Astron. Soc. **294**, 429 (1998).
[18] P. Ullio and M. Kamionkowski, J. High Energy Phys. 03 (2001) 049.
[19] We use the numerically calculated full axisymmetric VM potential in our MCMC analysis to find the Galactic model parameters. From this, we estimate that the error in the potential due to the spherical approximation at the solar location is ~9%, and the approximation gets increasingly better at larger r. The resulting errors in the normalized speed distribution give curves which still lie within the uncertainty bands (due to uncertainties of the rotation curve data) shown in Fig. 3.
[20] J. E. Taylor and J. F. Navarro, Astrophys. J. **563**, 483 (2001).
[21] M. Lisanti, L. E. Strigari, J. G. Wacker, and R. H. Wechsler, Phys. Rev. D **83**, 023519 (2011); P. J. Fox, G. D. Kribs, and T. M. Tait, Phys. Rev. D **83**, 034007 (2011); M. T. Frandsen, F. Kahlhoefer, C. McCabe, S. Sarkar, and K. Schmidt-Hoberg, J. Cosmol. Astropart. Phys. 01 (2012) 024.